Surface Layer Similarity under Nonuniform Fetch Conditions

A. C. M. BELJAARS, P. SCHOTANUS[1] AND F. T. M. NIEUWSTADT

Royal Netherlands Meteorological Institute, De Bilt, The Netherlands

(Manuscript received 12 February 1983, in final form 9 June 1983)

ABSTRACT

This paper discusses the results of a surface-layer experiment near the Cabauw meteorological mast. We measured momentum, heat and moisture fluxes at two heights, namely, 3.5 and 22.5 m. The measurements also include the mean wind speed and mean temperature profiles. The purpose was to investigate surface-layer similarity laws under nonideal fetch conditions. We found that under such conditions, the shear stress increases with height because of obstacles upstream. As a consequence flux-profile relationships differ from those over uniform terrain. It is shown that these deviations imply a slow relaxation in the exchange coefficient for heat and momentum over a terrain with changing surface roughness. Furthermore, we found that horizontal velocity fluctuations scale on a friction velocity representative of a large area. On the other hand, vertical velocity fluctuations scale on the local friction velocity.

1. Introduction

The Monin–Obukhov similarity theory is a well-established framework for presentation of meteorological data in the homogeneous atmospheric surface layer. The nondimensional relationships for the velocity and temperature gradients (cf. Dyer and Hicks, 1970; Businger *et al.*, 1971) are of particular interest since they can be used for practical estimates of heat and momentum fluxes from measured temperature and wind gradients. It should be noted, however, that different authors still find slightly different forms of these so-called "flux-profile relationships" (cf. Yaglom, 1977, and Viswanadham, 1982, for recent surveys).

In real situations the circumstances are often far from ideal; homogeneous fetch conditions over several thousands of meters are the exception rather than rule. The experimental data obtained at the KNMI 200 m meteorological tower at Cabauw also suffer from such nonideal fetch conditions. (cf. Nieuwstadt, 1978; Beljaars, 1982). Beljaars (1982) shows that a kink is present in the observed neutral wind profile at about 20 m height. This was attributed to different roughness conditions and obstacles in the upstream terrain, which lead to an increase of shear stress with height. Moreover the mean wind profile above 20 m suggests a larger z_0 than the profile near the surface. Comparable observations have been reported recently from the Boulder tower (Korrell *et al.*, 1982). Another effect which is often present in perturbed situations is a deviation of the well known flux-profile relationships for uniform terrain. This effect has been reported by Peterson (1969b) for a perturbed situation and by Garratt (1978) for measurements above an extremely rough surface and has also been predicted by Rao *et al.* (1974) and Peterson (1969a) on the basis of second order models. Simple integral models (for example, cf. Townsend, 1965) do not account for this.

Beljaars (1982) proposes that the deviation from the flux-profile relationships for homogeneous terrain is due to a very slow relaxation of the exchange coefficients from the upstream value (influenced by obstacles) to the value that is representative for the smooth measuring field. This conclusion could only be drawn from experimental data by making two assumptions, namely: 1) the heat flux in the surface layer is independent of height (this in contrast with the shear stress) and 2) in a perturbed situation the exchange coefficient for heat and momentum are modified in the same way.

The purpose of the present paper is to verify experimentally the assumptions previously mentioned. Furthermore, we investigate how the measured profiles and turbulence data, obtained for poor fetch conditions, can be presented within the Monin–Obukhov similarity theory for the ideal surface layer.

2. Experimental set-up

The data, presented here, were obtained near the 200 m meteorological mast in Cabauw. This tower is located in the center of the Netherlands in a flat area. The surface cover consists of grassland, interrupted by orchards, tree rows, small villages and ditches. The topographical details near the tower are

[1] Institute for Meteorology and Oceanography, University of Utrecht, Netherlands.

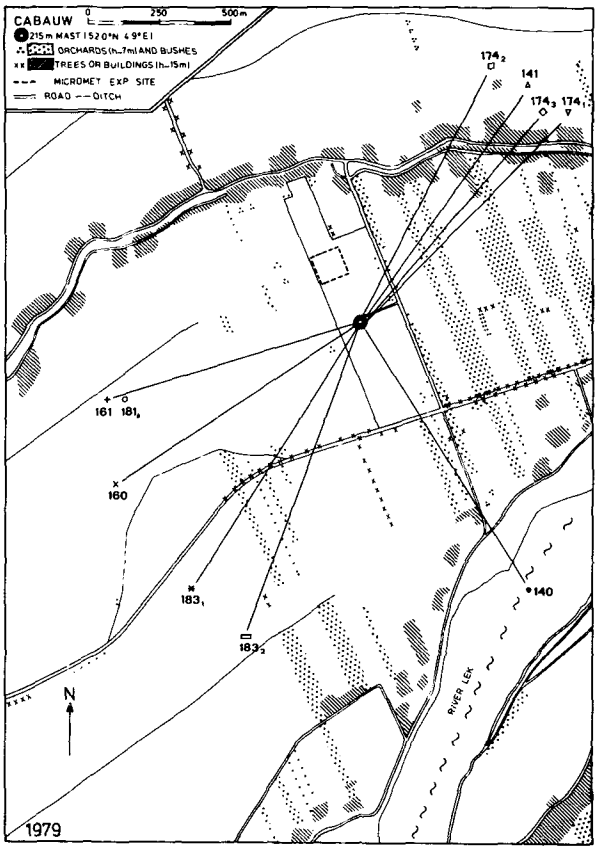

FIG. 1. Topography near the Cabauw meteorological mast. Day numbers are indicated at the end of lines that mark the wind direction during the different measuring runs.

illustrated in Fig. 1. The white area in this figure is grassland. This is also the ground cover in the immediate surroundings of the tower. In the southwest direction there is a narrow sector that is free from obstructions for several kilometers. For most other directions sparsely distributed obstacles are present; for easterly winds we can even speak of a transition from a rough to a smooth surface.

The main instrumentation during the experiment consists of turbulence sensors at 3.5 and 22.5 m height combined with sensors for mean wind and temperature in the same height range.

The turbulence equipment at 3.5 m height combines a three-component sonic anemometer, a fast thermocouple, a Lyman-alpha (Ly-α) humidity sensor and a constant temperature hot wire anemometer. With exception of the hot wire, all these sensors are located within a measuring volume with sides of about 20 cm. As checked in a wind tunnel, flow distortion is negligible. The sonic anemometer is a Kaijo–Denki DAT300 with a TR61A three dimensional wind probe which was pointed in the main wind direction by means of a manually controlled rotor. The thermocouple has a thickness of about 0.2 mm and a response time of about 0.2 s. The Lyman-alfa humidity sensor is manufactured by Electromagnetic Research Corporation (model BLR) and has a path length of 20 mm. The details of sonic anemometer calibration and flux measurements with Ly-α and thermocouple are given by Schotanus *et al.* (1983).

The measurements at 3.5 m height are supplemented by a hot wire anemometer in order to determine dissipation of turbulent kinetic energy. A single hot wire (diameter 5 μm, length 1 mm) was placed vertically. The signal was differentiated, squared and low-pass filtered by analog circuits before recording. In this way $\overline{(\partial u/\partial t)^2}$ could be measured; this was converted to $\overline{(\partial u/\partial x)^2}$ by means of Taylor's hypothesis (cf. Wyngaard and Coté, 1971). Although Taylor's hypothesis might be questionable in nonhomogeneous cases, it is still believed applicable at the end of the energy cascade in the dissipation range. The dissipation ϵ follows from $\epsilon = 15\nu\overline{(\partial u/\partial x)^2}$ which is based on the assumption that turbulence is isotropic in the dissipation range. This method is equivalent to the one used by Wyngaard and Coté (1971) and it works well except for low dissipation rates where electronic noise problems interfere (the noise level corresponds to a dissipation rate of the order of 0.01 $m^2 s^{-3}$).

At 22.5 m height a three-dimensional propeller vane (trivane) is used combined with thin (0.1 mm diameter) wet and dry thermocouples. The response lengths of the propeller and vane are 0.5 and 0.9 m, respectively, (Monna and Driedonks, 1979).

Mean temperature differences are measured by means of ventilated thermocouples at heights of 0.5, 2, 10 and 20 m. The mean wind is measured with Young 8002 *D* propeller vanes at 3, 6, 10 and 20 m height.

3. Fluxes in relation to profiles

The present data are based on measurements during 10 runs, each about 3 h duration. Each run represents different stability conditions and/or wind directions. Table 1 provides some general information on these periods. Variances and covariances are calculated as 30 min averages after removal of linear trends over 10 min intervals.

The presence of obstacles in the upstream terrain is most clearly seen as a height dependence of the friction velocity u_*, where $u_* = (\overline{-u'w'})^{1/2}$, $\rho\overline{u'w'}$ is the Reynolds shear stress and ρ air density. For most measuring periods, the friction velocity at 22.5 m height is about 40% larger than the friction velocity at 3.5 m height, as shown in Fig. 2. However, on day 160, 161 and 181, the ratio of friction velocities is about unity as it should be in the homogeneous surface layer. The connection of these results with topography becomes clear from Fig. 1 where the mean

TABLE 1. Summary of measuring periods.

Day number	Mean wind direction (deg)	Mean L (m)	Mean wind at 20 m (m s^{-1})	Remarks
140	148	−300	5.1	
141	36	−50	3.7	
160	236	−800	9.1	Almost no obstacles in the upstream terrain
161	253	−170	9.6	Almost no obstacles in the upstream terrain
174I	46	−16	2.3	
174II	27	+80	3.4	
174III	42	+16	3.1	
181	253	+3000	8.6	Almost no obstacles in the upstream terrain
183I	212	−135	5.3	
183II	200	−203	3.7	

wind direction is indicated for the different measuring periods. Only on day 160, 161 and 181 the wind is coming over a relatively obstacle-free area. It should also be noted that for the perturbed periods, the density of obstacles hardly influences the shear stress ratio between the two measuring levels.

In contrast to shear stress which is directly affected by obstacles and surface roughness, heat and moisture fluxes are not necessarily changed by the varying terrain. The present measurements show that they are not altered by the poor fetch conditions. In Figs. 3 and 4 heat and moisture fluxes at 3.5 and 22.5 m height are compared and no systematic flux increase or decrease can be observed.

We now consider the dimensionless wind shear and potential temperature gradient, defined as

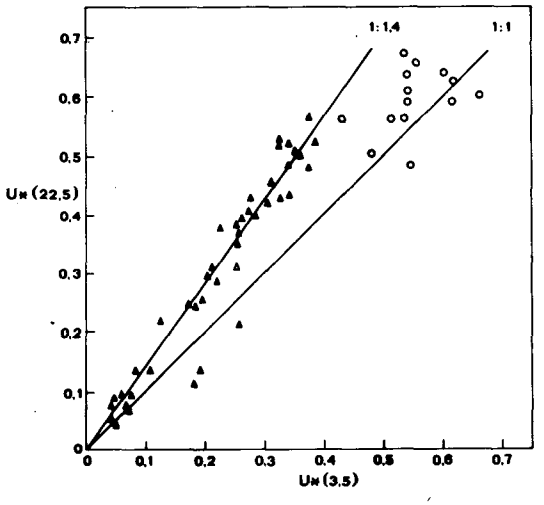

FIG. 2. Friction velocity at 22.5 m height as a function of friction velocity at 3.5 m height. Unperturbed measuring points are indicated by a circle; the perturbed ones by a triangle.

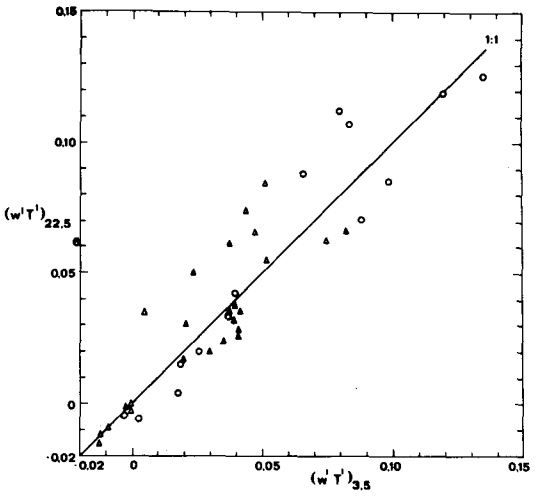

FIG. 3. Heat flux at 22.5 m height compared with heat flux at 3.5 m height for perturbed (△) and unperturbed (○) upstream terrain.

$$\left.\begin{aligned}\phi_m &= \frac{\partial \bar{u}}{\partial z}\frac{kz}{u_*}\\ \phi_h &= \frac{\partial \theta}{\partial z}\frac{kz}{\theta_*}\end{aligned}\right\}, \tag{1}$$

where $\theta_* = -\overline{w'T'}/u_*$ and $L = -Tu_*^3/(gk\overline{w'T'})$. These dimensionless values are calculated from the measured mean gradients and the measured turbulent fluxes as a function of z/L where L is based on the fluxes at the same level. Only the measurements from the 3.5 m level are used to calculate ϕ_m and ϕ_h. The value of the Von Karman constant has been taken equal to 0.4 which seems to be the value accepted by most researchers (cf. Yaglom, 1977; Wieringa, 1980). An

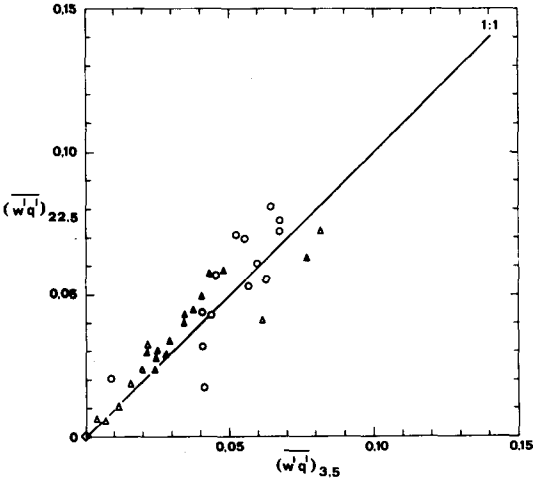

FIG. 4. As in Fig. 3, but for moisture flux.

effort has also been made to calculate ϕ_m and ϕ_h for the 22.5 measuring level, but the mean gradients are very small here. The resulting pictures showed too much scatter to draw any conclusions.

Windshear has been calculated by means of the velocity difference between 3 and 6 m on a logarithmic scale. It turns out that in neutral cases the 3, 6 and 10 m winds obey the logarithmic form very well, which means that incorporating the 10 m wind in the shear-calculating procedure would not have changed the results. Temperature gradients have been calculated by fitting a logarithmic profile through the 0.5, 2 and 10 m measuring points.

The dimensionless functions for wind and potential temperature gradient are shown in Figs. 5 and 6, respectively. Obviously it is not clear that such functions exist for nonhomogeneous terrain. In order to assess the influence of poor fetch conditions, we should like to compare it with empirical functions for uniform terrain. Much experimental effort has been made in the past to determine these functions and many forms have been proposed (cf. Yaglom, 1977 for a survey). Even the value of the Von Karman constant has been argued. Following Yaglom we select $k = 0.4$ and rescale the empirical functions proposed by Businger *et al.* (1971) and Dyer and Hicks (1970) to this value. This leads to slightly different constants in their analytic expressions. These functions are shown in the Figs. 5 and 6 by solid lines. When we restrict ourselves to the data points that correspond to the unperturbed wind directions, then it is clear that they match rather well with the Dyer and Hicks curve in Fig. 5 and that they are even below the Businger *et al.* curve in Fig. 6.

The ratio ϕ_h/ϕ_m in almost neutral conditions is about 0.7 which is in agreement with the results of the Kansas experiment (Businger *et al.*, 1971) and with Högström (1974), but in disagreement with the results of Dyer

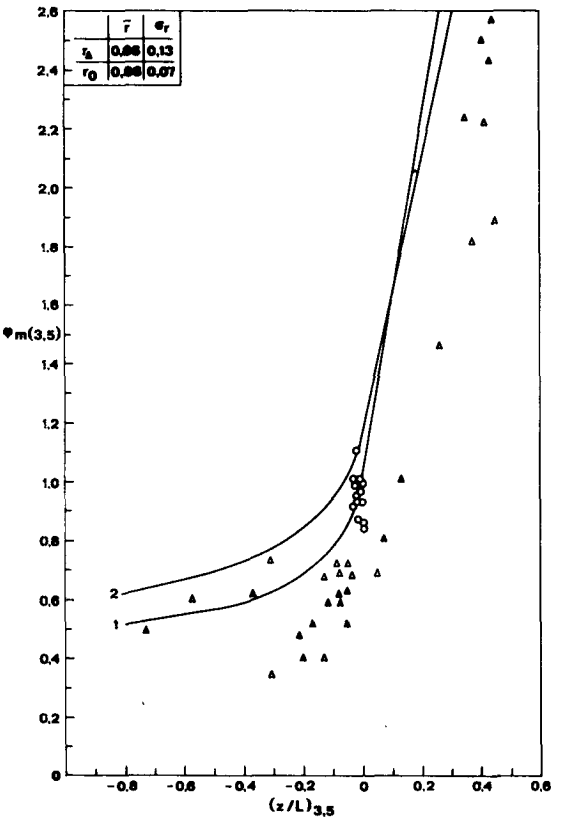

FIG. 5. Dimensionless windshear ϕ_m at 3.5 m height as a function of z/L. Perturbed (Δ) and unperturbed (O) fetch conditions are distinguished. The solid lines represent empirical functions from literature:

1) Dyer and Hicks (1970) with 0.98 $(1-16.4\ z/L)^{-1/4}$ for $z/L < 0$ and Kondo (cf. Yaglom, 1977) with $1 + 6\ z/L$ for $z/L > 0$;
2) Businger *et al.* (1971) with 1.14 $(1-13.1\ z/L)^{-1/4}$ for $z/L < 0$ and $1.14\ (1 + 4.1\ z/L)$ for $z/L > 0$.

Table insert: Mean value and standard deviation of the ratio between the observations and the calculation with function 2 for the unstable and neutral points only.

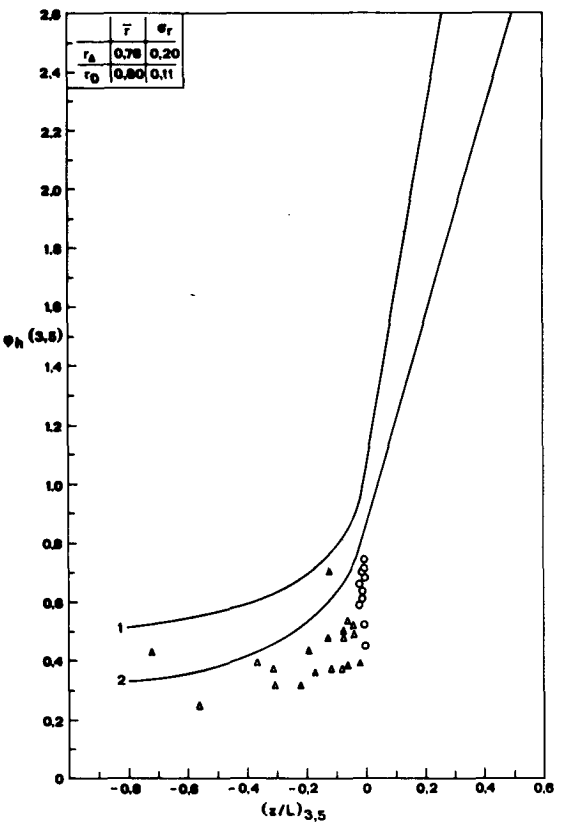

FIG. 6. Dimensionless potential temperature gradient ϕ_h at 3.5 m height as a function of z/L. Perturbed (Δ) and unperturbed (O) fetch conditions are distinguished. The solid lines represent empirical functions from literature: 1) Dyer and Hicks (1970) with $0.98\ (1 - 16.4\ z/L)^{-1/4}$ for $z/L < 0$ and Kondo (cf. Yaglom, 1977) with $1 + 6\ z/L$ for $z/L > 0$; 2) Businger *et al.* (1971) with $0.84\ (1 - 7.9\ z/L)^{-1/2}$ for $z/L < 0$ and $1.14\ (0.74 + 4.1\ z/L)$ for $z/L > 0$. The numbers in the table have been calculated as in Fig. 5.

and Hicks (1970) and those of Dyer and Bradley (1982) who found unity for this ratio.

The measured values for ϕ_m and ϕ_h that correspond to perturbed wind directions are systematically below the curves for uniform terrain. This was also found by Peterson (1969b) and Garratt (1978). In Beljaars (1982), it has been concluded that the exchange coefficient for momentum and heat should scale on the friction velocity at 22.5 m height instead of the local value. Two assumptions had to be made to arrive at this conclusion, namely: 1) the ratio ϕ_m/ϕ_h is not altered by perturbations and 2) heat flux does not change with height. Since both assumptions seem to be justified by present results, the conclusion that the exchange coefficients scales on $u_*(22.5)$ should hold. Therefore, instead of

$$\left(\frac{K}{u_* kz}\right)_{3.5} = \frac{1}{\phi_{m,h}} = F\left(\frac{z}{L}\right), \tag{2}$$

where K is the exchange coefficient we write

$$\frac{K(3.5)}{u_*(22.5)kz} = \frac{1}{\left(\frac{u_*(22.5)}{u_*(3.5)}\right)\phi_{m,h}} = G\left(\frac{z}{L}\right), \tag{3}$$

where $\phi_{m,h}$ are obtained from (1). The scaling behavior as indicated by (3) can be verified by plotting

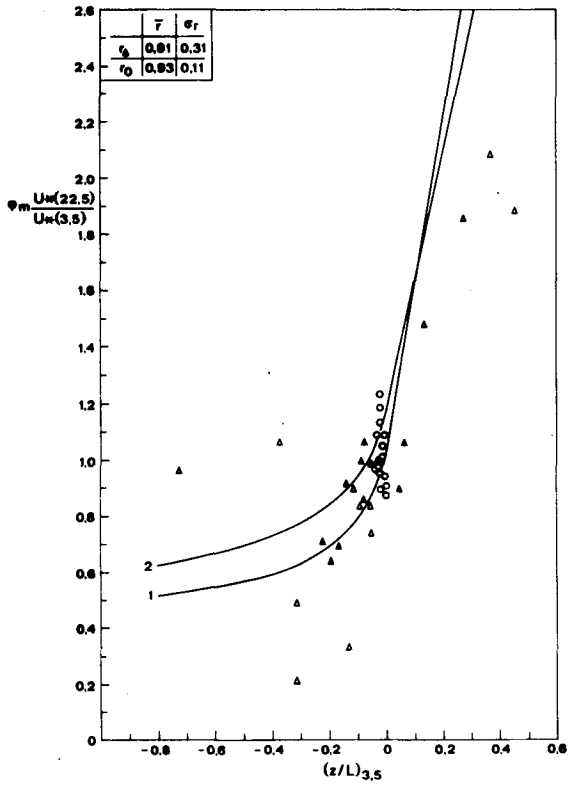

FIG. 7. The dimensionless wind shear multiplied by the ratio $u_*(22.5)/u_*(3.5)$. Symbols and lines as in Fig. 5.

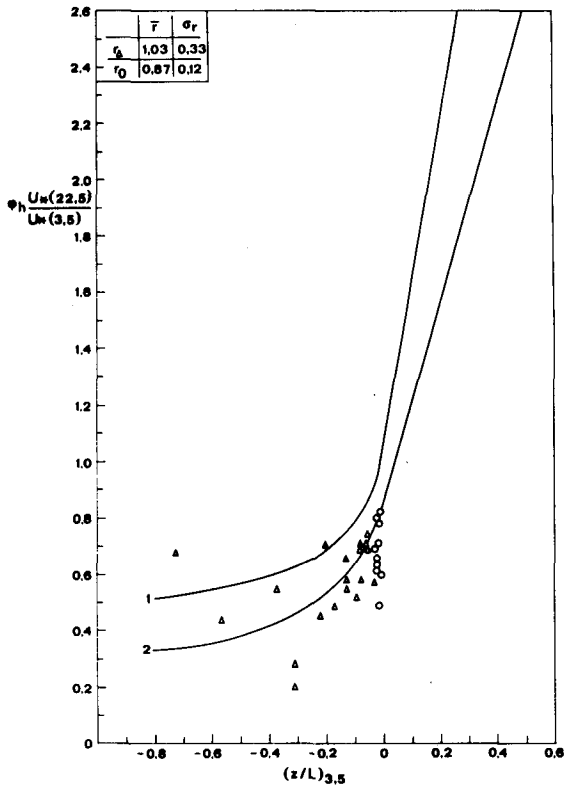

FIG. 8. The dimensionless potential temperature gradient multiplied by $u_*(22.5)/u_*(3.5)$. Symbols and lines as in Fig. 6.

u_* (22.5) ϕ/u_* (3.5) as a function of z/L (cf. Figs. 7 and 8; z/L has been calculated for the 3.5 m measuring level). As a result of this procedure, the measuring points corresponding to the perturbed situation, change by a factor 1.4 on the average.

Although the scatter increases considerably by this procedure, the systematic difference between perturbed and unperturbed points has disappeared now in ϕ_m. The measured value of ϕ_h and ϕ_m, plotted in this way, agree much better with the well established empirical functions (Dyer and Hicks, 1970; Businger *et al.*, 1971). It should be noted however that most of the ϕ_h measurements were done with very small heat-flux-values, which implies rather large scatter due to measuring errors.

The following interpretation can be given to the unusual scaling behavior as expressed by (3). The 22.5 m measuring level shows the integrated effect of a large upstream area. The shear stress measured here includes the form drag on obstacles far away and therefore it is larger than the local surface drag. At 3.5 m height, the shear stress tends towards the surface drag on the smooth measuring terrain. The exchange coefficient, however, has still the value that corresponds to a large area, including the obstacles upstream. Apparently, relaxation in the exchange coefficient is very slow.

Although a complex terrain (Fig. 1) can hardly be represented by a model, it is still interesting to compare some of the present results with calculations done by Rao *et al.*, (1974) for the "step in roughness problem." We concentrate on the following two questions; over which height range does the shear stress vary with height and where can nonequilibrium between fluxes and profiles ($\phi_m \neq 1$ for neutral flow) be expected? First of all we have to choose representative values for the distance between measuring position and the rough-to-smooth transition and for the magnitude of the roughness transition. As a characteristic distance to the nearest obstacles we take about 500 m; for the ratio of roughness lengths we choose 10 (0.20 m/0.02 m). For these parameters Rao *et al.*, (1974) predict a vertical length scale λ of about 12 m at the measuring location with the main variation of stress between 0.5 λ = 6 m and 2 λ = 24 m height. This means that our 3.5 m measuring level should produce the surface shear stress, whereas the 22.5 m stress measurement should be very close to the upstream stress. The situation is different for function ϕ_m. This function deviates from 1 between 0.1 λ = 1.2 m and 2 λ = 24 m. This means that our lowest stress measuring point at 3.5 m feels nonequilibrium effects, as we have shown in Figs. 5 and 6. In conclusion, we can say that the model predictions by Rao *et al.*, (1974) agree at least qualitatively with the measurements.

4. The energy budget

In the adjustment of the flow to a new boundary condition behind a roughness change, the turbulent energy budget plays an important role. The importance of the equation for turbulent energy is stressed by several modelers with the argument that it accounts for the local nonequilibrium between fluxes and mean gradients (cf. Peterson, 1972). Rao *et al.* (1974) even argue that an equation for the turbulent length scale or for disspation of turbulent energy is needed for this problem.

The equation for turbulent energy E reads

$$\frac{dE}{dt} = -\overline{u'w'}\frac{\partial \bar{u}}{\partial z} + \frac{g}{T}\overline{w'T'} - \frac{\partial}{\partial z}\overline{w'\left(E + \frac{p'}{\rho}\right)} - \epsilon,$$

where

$$E = \tfrac{1}{2}(\overline{u'^2} + \overline{v'^2} + \overline{w'^2}).$$

The different terms at the rhs of this equation represent, respectively, the production by shear, the production by buoyancy, the diffusion by vertical velocity and pressure fluctuations, and dissipation. At the 3.5 m level, three terms have been measured directly in the present experiment; namely, shear production, buoyancy production and dissipation. The sum of the two production terms is compared in Fig. 9 with the dissipation. Within the usual scatter, no systematic nonequilibrium can be observed between production and dissipation. In addition, no systematic effect can be deduced when perturbed and unperturbed fetch conditions are distinguished. This result supports Peterson's (1972) conclusion that as a rough estimate, production equals dissipation and that turbulent diffusion accounts for advection. This experimental result however has implications for the complexity of the model needed to deal with the present problem. If we define $\epsilon = u_t^3/l$ where u_t and l stand for a turbulent velocity and length scale, we can express the statement that production equals dissipation for neutral conditions as follows:

$$\frac{u_*^3}{kz}\phi_m(0) = \frac{u_t^3}{l}.$$

In case of unperturbed flow, the turbulent velocity scale will be u_* and the length scale kz. We have seen, however, that due to perturbations, $\phi_m(0)$ deviates from 1 and has a value of about $u_*(3.5)/u_*(22.5)$. It is not clear now whether u_t should be adjusted or l. When we choose $u_t = u_*$ as Peterson (1969a), we have to conclude that $l > kz$ inside the internal boundary layer, which is inconsistent with Peterson's second assumption, namely, $l = kz$. A dynamic equation for the length scale seems necessary in such cases.

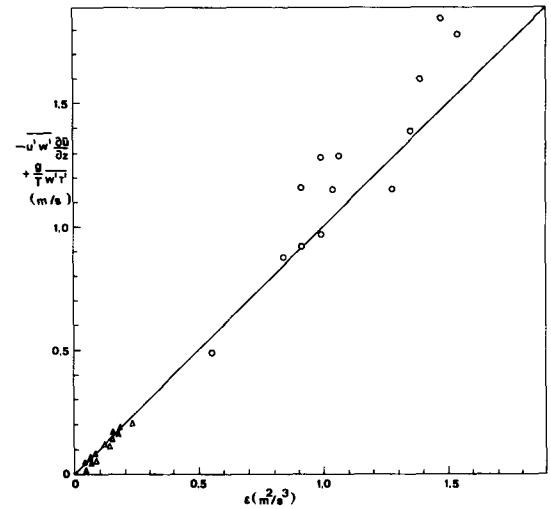

FIG. 9. Measured shear production added to buoyancy production as a function of measured dissipation (O unperturbed fetch; Δ perturbed fetch).

5. The turbulence intensities

In this section the scaling behavior of turbulence variances is investigated for its dependence on fetch conditions. Following the procedure used for u_*, we compare σ_u and σ_w at the two measuring levels (cf. Figs. 10 and 11). It is clear from Fig. 10 that the shear

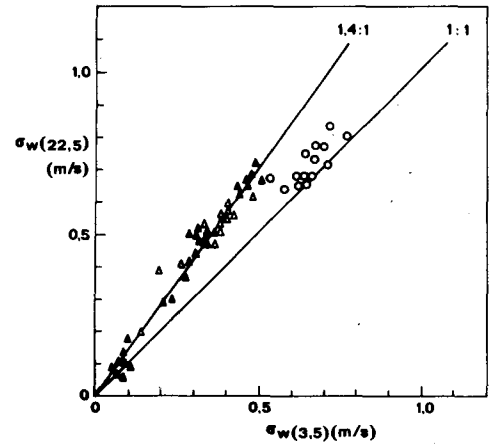

FIG. 10. Standard deviation of the w-component at 22.5 m in comparison with this parameter at 3.5 m. (O unperturbed fetch; Δ perturbed fetch).

stress increase with height for the perturbed cases is also reflected in σ_w. On the other hand, we do not observe any systematic effect in σ_u (cf. Fig. 11). These results strongly suggest scaling of σ_w on the local u_* and scaling of σ_u at both heights on the same u_* value. For the latter, we choose the friction velocity at 22.5 m height. The idea behind this is that the low frequency part of σ_u contributes considerably to σ_u and adjusts very slowly to the new shear stress. This part of the turbulence spectrum is often called inactive, since it contributes at low heights only to the horizontal components but does not have any transport properties. This distinction between active and inactive turbulence was introduced by Townsend (1961; cf. also Bradshaw, 1967) and applied to atmospheric flow by Panofsky *et al.* (1977). The latter authors show that the low frequency part of the horizontal velocity components do not obey surface layer scaling. In the case of changing surface conditions the

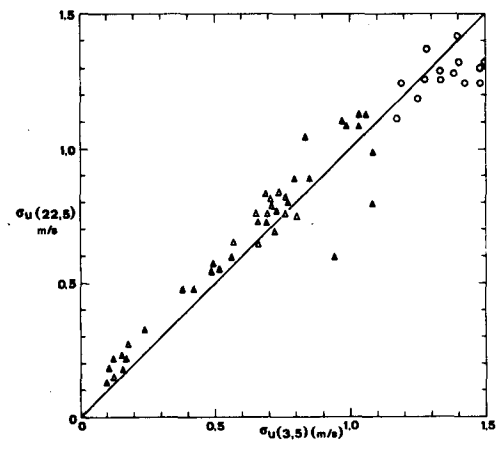

FIG. 11. As in Fig. 10 but for the u-component.

largest scales contribute considerably to the horizontal components and adapt very slowly to the local stress. The large scale part of the fluctuations carries the characteristics of the upstream terrain, and therefore scales on the friction velocity that is representative for a large terrain. This was also concluded by Panofsky *et al.* (1982) who investigated the spectral behavior of turbulent fluctuations over complex terrain.

We now apply the presumed scaling behavior to the data. One of the problems is the definition of the stability parameter z/L. Use of the local stress in order to calculate Monin-Obukhov length seems the most obvious choice. When z/L is interpreted as the ratio of buoyancy and shear production, this can be in error by a factor of $u_*(22.5)/u_*(3.5)$ (about 1.4 in the present experiment). In the free convection limit, this problem can be ignored since scaling becomes independent of friction velocity. Moreover most empirical functions for turbulent quantities depend only weakly on z/L which makes the accuracy of the stability parameter less important. The dimensionless variances for the u, v and w-components are shown in Figs. 12, 13 and 14 for both measuring levels. The variances σ_u and σ_v are scaled on $u_*(22.5)$ for the observations of 3.5 m height, as well as of 22.5 m height; local scaling has been applied to σ_w.

In general, it can be concluded that the present results for the inhomogeneous surface layer (scaled on the "global" u_* for the u and v-components and on the "local" u_* for the w-component) agree well with the results for the homogeneous surface layer (cf. Busch, 1973, for a survey). The neutral value of 2.3 for σ_u/u_* found by McBean (1971) is slightly larger than the value 2 found in the present experiment (cf. Fig. 12). McBean (1971) found $\sigma_v/u_* = 1.7$ which compares well with the results shown in Figs. 12 and 13. The uncertainty in these variables is large: Wyngaard and Coté (1974) suggest 2 and 1.75 for σ_u/u_* and σ_v/u_*, respectively, on the basis of the Kansas experiment; Hicks (1981) found 2.25 and 1.9 after reanalysis of these data. Although Figs. 12 and 13 clearly suggest surface layer scaling, the results might as well scale on z_i/L (z_i stands for boundary layer height) as suggested by Panofsky *et al.* (1977). This will be especially important for large instability where our data show most of the scatter.

The σ_w/u_* values measured at 3.5 m and 22.5 height plot over each other with relatively small scatter; they clearly obey Monin–Obukhov similarity. The data points stay slightly below the empirical function given by Wyngaard and Coté (1974) (cf. Fig. 14).

The results for $\sigma_T/\|\theta_*\|$ and σ_q/q_* as shown in Figs. 15 and 16 clearly obey the expected "$-\frac{1}{3}$" power law for free convection. Scaling on local fluxes has been applied here as a working hypothesis although the justification is not clear for this. The measurements agree well with $\sigma_T/\|\theta_*\| = 0.95\|z/L\|^{-1/3}$ as found by Wyn-

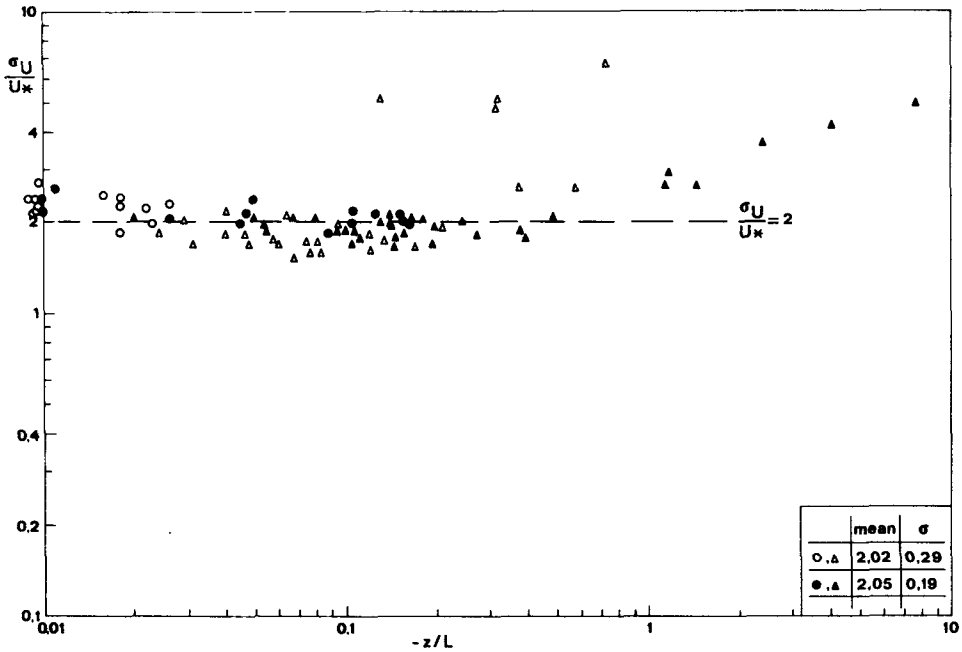

FIG. 12. Measured σ_u/u_* as a function of z/L for both heights. The measured u_* value at 22.5 m height has been applied as scaling for both measuring levels of σ_u. Open symbols corresponds to 3.5 m; closed to 22.5 m. (open and solid triangles for perturbed fetch; open and solid circles for unperturbed fetch). Table insert: The mean value and the standard deviation of σ_u/u_* calculated for $0 < -z/L < 0.2$. The mean value of $\sigma_u/u_* = 2.56$ for the 3.5 m level when local scaling is applied.

gaard *et al.* (1971) and with $\sigma_q/q_* = 1.04\|z/L\|^{-1/3}$ as suggested by Högström (1974). The near neutral value, which is very difficult to measure because of the small fluxes, is about 3.5 for $\sigma_T/\|\theta_*\|$ and about 2.5 for σ_q/q_*. This agrees with Tilmann (1972) who also found $\sigma_T/\|\theta_*\| = 3.5$ as neutral limit.

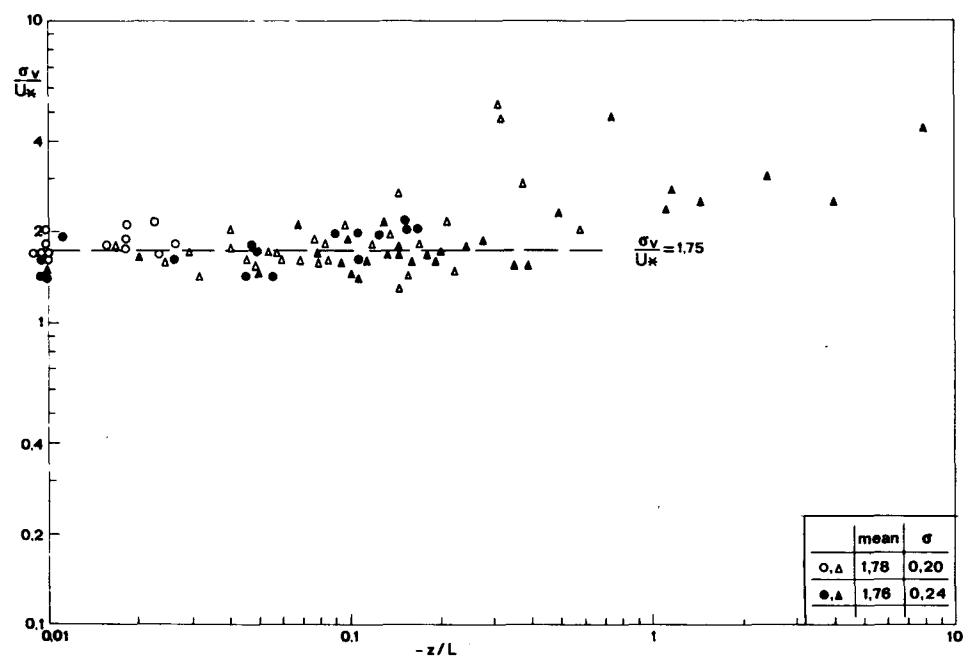

FIG. 13. Measured σ_v/u_* as a function of z/L. Scaling and symbols as in Fig. 12. Local scaling at 3.5 m height leads to a mean value for σ_v/u_* of 2.29.

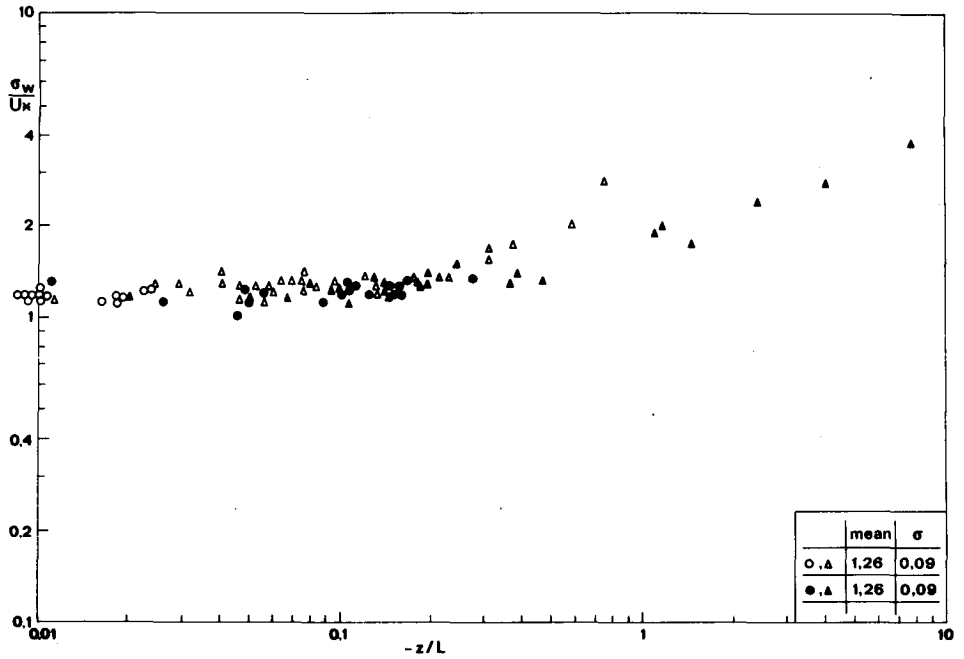

FIG. 14. Measured σ_w/u_* as a function of z/L. Local scaling has been applied. Symbols as in Fig. 12.

6. Conclusions

Surface layer observations of mean profiles and turbulence quantities have been presented. The observations are typical of an agricultural site which is not completely uniform but represents regions with enhanced roughness. Even the sparsely distributed obstructions near the experimental site lead to a considerable shear stress increase with height whereas heat and moisture fluxes show no variance. As a result, the flux profile relationships for uniform terrain are not applicable in such situations. The exchange

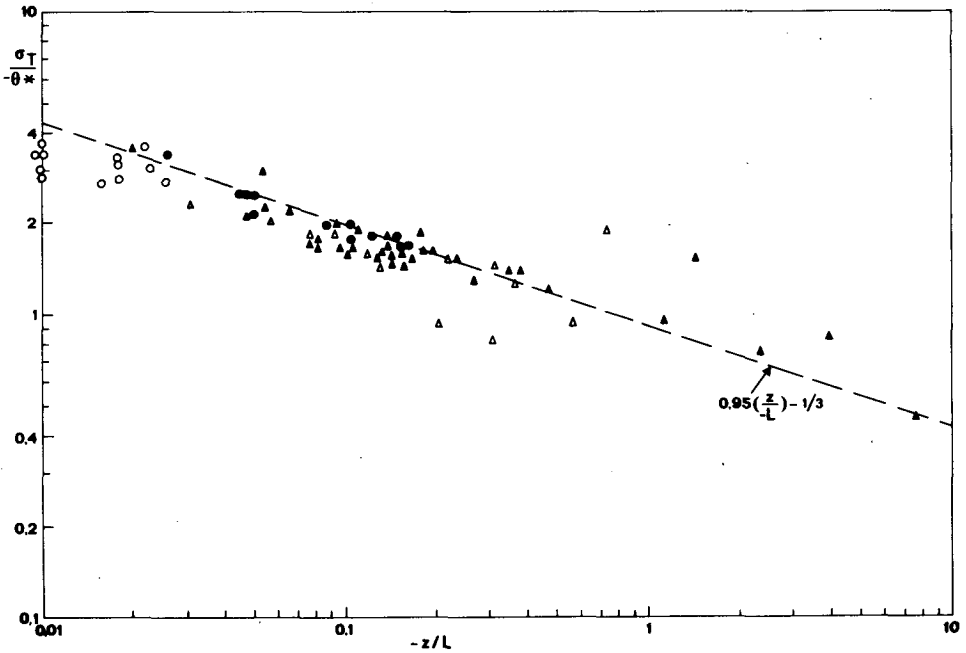

FIG. 15. Intensity of temperature fluctuations scaled on the local θ_* as a function of z/L for two measuring levels. Symbols as in Fig. 12.

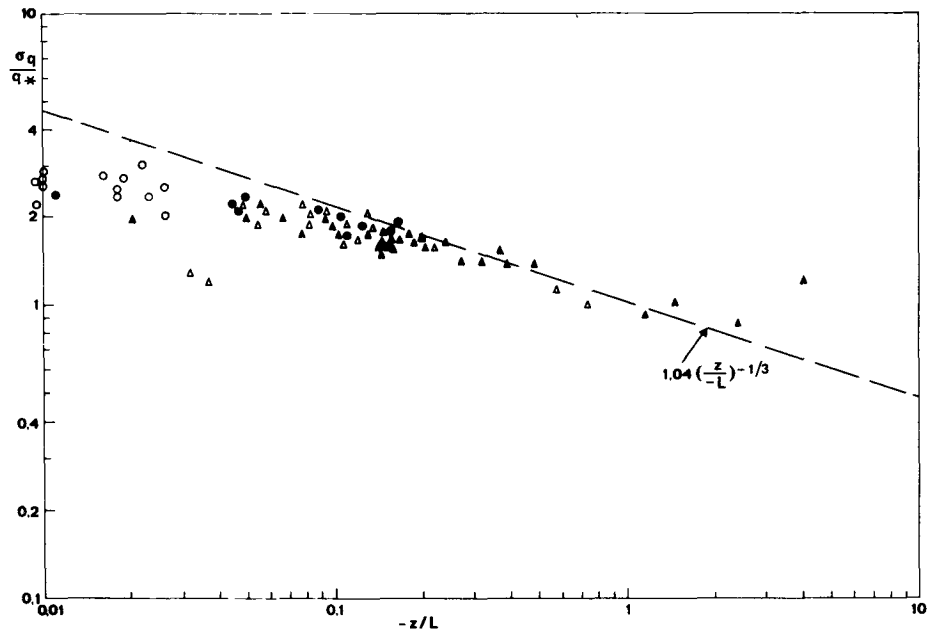

FIG. 16. Intensity of humidity fluctuations scaled on the local q_* as a function of z/L for two measuring levels. Symbols as in Fig. 12.

coefficients for momentum and heat turn out to scale on the friction velocity that is representative of a large area, the inclusion of a correction factor leads to closer agreement.

As far as the turbulence intensities are concerned, we have to distinguish between the u and v component and other quantities. The u and v fluctuations bear the characteristics of a large area that not only includes the relatively smooth terrain near the measuring point but also the obstacles upstream. As a result the variances of the u and v fluctuations are independent of height and scale on the friction velocity that is representative of a rather large terrain upstream. The vertical velocity fluctuations, however, scale on the local friction velocity. The σ_w values also increase with height for the wind directions with obstacles in the upstream area. Application of this scaling (global scaling for σ_u and σ_v and local scaling for σ_w) leads to empirical functions of z/L that do not differ significantly from those found in the literature for uniform terrain. Local scaling also seems valid for temperature and humidity fluctuations.

The global scaling of σ_u, independent of measuring height, is very useful in applications where one is interested in the shear stress averaged over a large area. In such cases, it is sufficient to measure σ_u, apply the empirical function in order to obtain global friction velocity. This method is not affected by terrain irregularities or poor fetch conditions.

Acknowledgment. The authors thank the Instrumental Department of the KNMI. Without their support this experiment would not have been possible.They are also indebted to Dr. W. Oost for his kindness in lending the sonic anemometer for this experiment.

REFERENCES

Beljaars, A. C. M., 1982: The derivation of fluxes from profiles in perturbed areas. *Bound.-Layer Meteor.*, **24**, 35–55.

Bradshaw, P., 1967: "Inactive" motion and pressure fluctuations in turbulent boundary layers. *J. Fluid Mech.*, **30**, 241.

Busch, N. E., 1973. The surface boundary layer, Part I. *Bound.-Layer Meteor.*, **4**, 213–240.

Businger, J. A., J. C. Wyngaard, Y. Izumi and E. F. Bradley, 1971: Flux-profile relationships in the atmospheric surface layer. *J. Atmos. Sci.*, **28**, 181–189.

Dyer, A. J., and B. B. Hicks, 1970: Flux-gradient relationships in the constant flux layer. *Quart. J. Roy. Meteor. Soc.*, **96**, 715–721.

——, and E. F. Bradley, 1982: An alternative analysis of flux-gradient relationships at the 1976 ITCE, *Bound.-Layer Meteor.*, **22**, 3–19.

Garratt, J. R., 1978: Flux profile relations above tall vegetation, *Quart. J. Roy. Meteor. Soc.*, **104**, 199–211.

Hicks, B. B., 1981: An examination of turbulence statistics in the surface boundary layer, *Bound.-Layer Meteor.*, **21**, 389–402.

Högström, U., 1974: A field study of the turbulent fluxes of heat, water vapour and momentum at a "typical" agricultural site. *Quart. J. Roy. Meteor. Soc.*, **100**, 624–639.

Korrell, A., H. A. Panofsky and R. J. Rossi, 1982: Wind profiles at the Boulder tower. *Bound.-Layer Meteor.*, **22**, 295–312.

McBean, G. A., 1971: The variations of the statistics of wind, temperature and humidity fluctuations with stability. *Bound.-Layer Meteor.*, **1**, 438–457.

Monna, W. A. A., and A. G. M. Driedonks, 1979: Experimental data on the dynamic properties of several propeller vanes. *J. Appl. Meteor.*, **18**, 699–702.

Nieuwstadt, F., 1978: The computation of the friction velocity u_*

and the temperature scale T_* from temperature and wind velocity profiles by least square methods, *Bound.-Layer Meteor.*, **14,** 235–246.

Panofsky, H. A., H. Tennekes, D. H. Lenschow and J. C. Wyngaard, 1977: The characteristics of turbulent velocity components in the surface layer under convective conditions, *Bound.-Layer Meteor.*, **11,** 355–361.

Peterson, E. W., 1969a: Modification of mean flow and turbulent energy by a change in surface roughness under conditions of neutral stability. *Quart. J. Roy. Meteor. Soc.*, **95,** 561–575.

——, 1969b: On the relation between the shear stress and the velocity profile after a change in surface roughness. *J. Atmos. Sci.*, **26,** 773–774.

——, 1972: Relative importance of terms in the turbulent energy and momentum equations as applied to the problem of a surface roughness change. *J. Atmos. Sci.*, **29,** 1470–1476.

Rao, K. S., J. C. Wyngaard and O. R. Coté, 1974: The structure of a two-dimensional internal boundary layer over a sudden change of surface roughness. *J. Atmos. Sci.*, **31,** 738–746.

Schotanus, P., F. T. M. Nieuwstadt and H. A. R. de Bruin, 1983: Temperature measurement with a sonic anemometer and its application to heat and moisture fluxes. *Bound.-Layer Meteor.*, **26,** 81–93.

Tillman, J. E., 1972: The indirect determination of stability, heat and momentum fluxes in the atmospheric boundary layer, from simple scalar variables during dry unstable conditions. *J. Appl. Meteor.*, **11,** 783–792.

Townsend, A. A., 1961: Equilibrium layers and wall turbulence. *J. Fluid Mech.*, **11,** 97.

——, 1965: The response of a turbulent boundary layer to abrupt changes in surface conditions. *J. Fluid Mech.*, **22,** 799–822.

Viswanadham, Y., 1982. Examination of the empirical flux-profile models in the atmospheric surface boundary layer. *Bound.-Layer Meteor.*, **22,** 61–77.

Wieringa, J., 1980: A reevaluation of the Kansas mast influence on measurements of stress and cup anemometer overspeeding. *Bound.-Layer Meteor.*, **18,** 411–430.

Wyngaard, J. C., and O. R. Coté, 1971. The budgets of turbulent kinetic energy and temperature variance in the atmospheric surface layer. *J. Atmos. Sci.*, **28,** 190–201.

——, and ——, 1974: The evolution of a convective planetary boundary layer—a higher order—closure model study. *Bound.-Layer Meteor.*, **7,** 289–308.

——, —— and Y. Izumi, 1971: Local free convection similarity and the budgets of shear stress and heat flux, *J. Atmos. Sci.*, **28,** 1171–1182.

Yaglom, A. M., 1977: Comments on wind and temperature flux-profile relationships, *Bound.-Layer Meteor.*, **11,** 89–102.